Equivalent Step Structures along Inequivalent Crystallographic Directions on Halogen-Terminated Si(111)-(1 × 1) Surfaces

B. S. Itchkawitz,* M. T. McEllistrem, and John J. Boland†

Department of Chemistry, University of North Carolina at Chapel Hill, Venable Hall, CB No. 3290, Chapel Hill, North Carolina 27599

(Received 23 August 1996)

Steps in inequivalent crystallographic directions are usually assumed to have different atomic structures. However, this Letter demonstrates that bilayer steps in the two principal crystallographic directions ($\langle \bar{1}\,\bar{1}2\rangle$ and $\langle 11\bar{2}\rangle$) of the Br-terminated Si(111)-(1 × 1) surface have the *same* atomic edge structure, due to the introduction of stacking faults along the $\langle 11\bar{2}\rangle$ step edges. Similar results are also observed for Cl- and I-terminated Si(111) surfaces. This strong preference for a particular step edge structure determines the surface morphology of steps, islands, and etch pits, and has profound ramifications for dry etching and chemical vapor deposition growth for this system. [S0031-9007(96)02002-9]

PACS numbers: 61.16.Ch, 68.35.Bs, 73.20.At, 82.65.My

It is well established that surface steps along different symmetry directions have different atomic structures. In this Letter, we present a study of the step structures on the Br-terminated Si(111)-(1 × 1) surface. This surface is prototypical of the larger silicon-halogen system, perhaps the most important chemical system in semiconductor processing. Remarkably, we find that steps along the inequivalent $\langle \bar{1}\,\bar{1}2\rangle$ and $\langle 11\bar{2}\rangle$ symmetry directions have the *same* step edge structure. This preferred structure is shown to have profound ramifications for dry etching [1] and chemical vapor deposition (CVD) growth [2–4] of Si(111) substrates, reflecting the critical role of surface steps in material processing.

Halogen-terminated Si(111)-(1 × 1) surfaces were prepared by exposing clean Si(111)-(7 × 7) surfaces at elevated temperatures (400–500 °C) to a flux of halogen molecules from an electrochemical cell [1,4–6]. Similar results were obtained for all halogens studied (Cl-, Br-, and I-terminated surfaces), and this work focuses on the Br termination as being representative. By varying the sample temperature during Br_2 exposure, the fraction of the surface converted from (7 × 7) to (1 × 1) can be varied from 0% to nearly 100% [4]. The (7 × 7) → (1 × 1) transformation occurs predominantly along steps [4], so that the atomic structure of the halogenated Si(111)-(1 × 1) surface steps can be examined even when the surface is not fully transformed to the (1 × 1) structure.

On the Br-terminated Si(111)-(1 × 1) surface, there are two primary types of single bilayer steps which have opposite orientations. Idealized structures for these surface steps are shown schematically in Fig. 1(a). By virtue of the two inequivalent atoms of the Si bilayer, there are two different step terminations possible for each step direction. Steps with their outward normals along the $\langle \bar{1}\,\bar{1}2\rangle$ set of directions (labeled $\langle \bar{1}\,\bar{1}2\rangle$ steps) may be terminated in one of two ways, each of which has Si atoms with two Si-Si bonds and two dangling bonds. If the step is terminated by the lower Si atoms of the bilayer (with their dangling bonds along the step edge), then dimerization along the step edge is expected [1]. However, if the upper Si atoms terminate these steps, the two dangling bonds are perpendicular to the step edge. These dangling bonds must be tied up in some manner, but there is insufficient room to accommodate singly coordinated Br atoms at all the dangling bonds near the step edge. Figure 1(a) shows a rebonded step geometry where the step-terminating Si atoms are bonded to Si atoms in the bottom terrace (*A*-type step

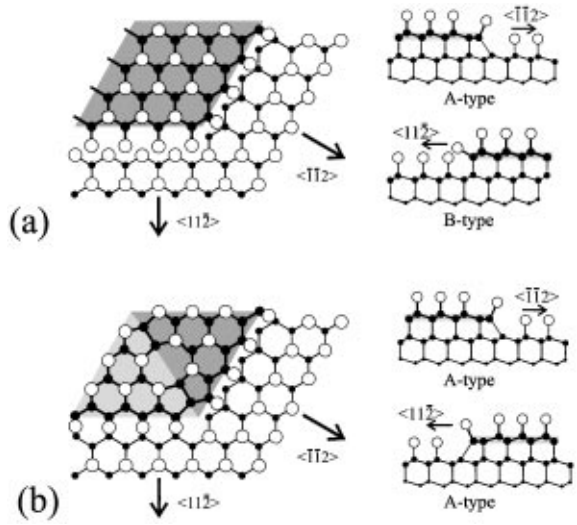

FIG. 1. Top- and side-view schematics of the atomic structure of the $\langle \bar{1}\,\bar{1}2\rangle$ and $\langle 11\bar{2}\rangle$ step edges for the Br-terminated Si(111)-(1 × 1) surface. For clarity, underlying atoms are not shown in the top views. White circles represent Br atoms, dark circles represent Si atoms, and gray areas denote the top terrace. (a) Step structures corresponding to an idealized bulklike termination with two different step structures along the two crystallographic directions; (b) step structures consistent with the observed STM images in which the two crystallographic directions have the same atomic structure.

 0031-9007/96/78(1)/98(4)$10.00 © 1996 The American Physical Society

edge). A similar structure has been proposed previously for $\langle \bar{1}\,\bar{1}2\rangle$ steps on the *H*-terminated Si(111)-(1 × 1) surface [7]. Alternatively, there may be a doubly coordinated Br atom occupying the bridging site between these two Si atoms. Steps with outward normals along the $\langle 11\bar{2}\rangle$ set of directions ($\langle 11\bar{2}\rangle$ steps) are shown in Fig. 1(a) as being terminated by the lower Si atoms of the bilayer, each of which has three Si-Si bonds and a single dangling bond, the latter being tied up by a single Br atom (*B*-type step edge). The alternative termination of $\langle 11\bar{2}\rangle$ steps involves the upper Si atoms of the bilayer, but it is expected to be less stable since these Si atoms have just one Si-Si bond and three dangling bonds.

As Fig. 1(a) shows, the atomic step edge structures of the (111)-(1 × 1) surface should then be dependent on the step orientation. Steps meandering across the surface are composed of $\langle \bar{1}\,\bar{1}2\rangle$ and $\langle 11\bar{2}\rangle$ step segments which define various kinks along the steps. For the ideal (111)-(1 × 1) surface, a 120° kink (one with a 120° change of the step's outward normal) has both step segments in the same set of crystallographic directions, and so it has the same edge structure along its two step segments. However, a 60° kink [with outward normals 60° different as shown in Fig. 1(a)] requires a change in crystallographic direction and therefore a change of the step edge structure.

Figure 2 illustrates atomically resolved STM images of single bilayer steps of the Br-terminated Si(111)-(1 × 1) surface, prepared using an exposure temperature of ~400 °C. Remarkably, triangular faulted structures of various sizes are observed along all $\langle 11\bar{2}\rangle$ step edges. These faulted structures are brighter than the surrounding bulk terminated structure due to the presence of a stacking fault [5,6], and are bounded by dimer rows [4,7]. In addition, faulted triangular structures have their apexes pointing in the $\langle \bar{1}\,\bar{1}2\rangle$ directions, as required by the crystallographic symmetry. The orientation of the faulted triangles therefore serves as a reminder of the crystallographic directions over the whole surface. $\langle 11\bar{2}\rangle$ step segments larger than four atoms in length have not been observed without being dressed by faulted structures. These faulted structures are not untransformed remnants of the original (7 × 7) structure since they usually have sizes different than the six atoms per side expected for faulted triangular half-cells of the (7 × 7) structure.

Surprisingly, both the $\langle 11\bar{2}\rangle$ and $\langle \bar{1}\,\bar{1}2\rangle$ steps have the *same* atomic edge structure [8], as is clearly evident in the inset of Fig. 2(c). Close scrutiny reveals no evidence for dimerization along the $\langle \bar{1}\,\bar{1}2\rangle$ steps, ruling out the possibility of $\langle \bar{1}\,\bar{1}2\rangle$ step termination by the bilayer's lower Si atoms. Furthermore, STM images show that the step edge atoms are lower than the atoms of the top terrace, and the edge atoms are separated from the terrace somewhat, yielding a shelflike appearance. These observations are consistent with the *A*-type edge structure shown in Fig. 1, in which Si rebonding at the step edge tilts the last Si atom of the top terrace downward toward the bottom terrace [9].

The equivalence of step edge structures for both step orientations is a consequence of the stacking faults which dress $\langle 11\bar{2}\rangle$ steps. Topologically, stacking faults that dress $\langle 11\bar{2}\rangle$ step edges exactly cancel the change of atomic edge structure across a 60° kink, as shown in Fig. 1(b). These faulted structures persist up to exposure temperatures at which Br desorption occurs (~800 °C), where nearly the entire surface has a bulklike (1 × 1) structure. These results strongly suggest that it is energetically favorable to maintain *A*-type rather than *B*-type atomic edge structures along $\langle 11\bar{2}\rangle$ steps, despite the

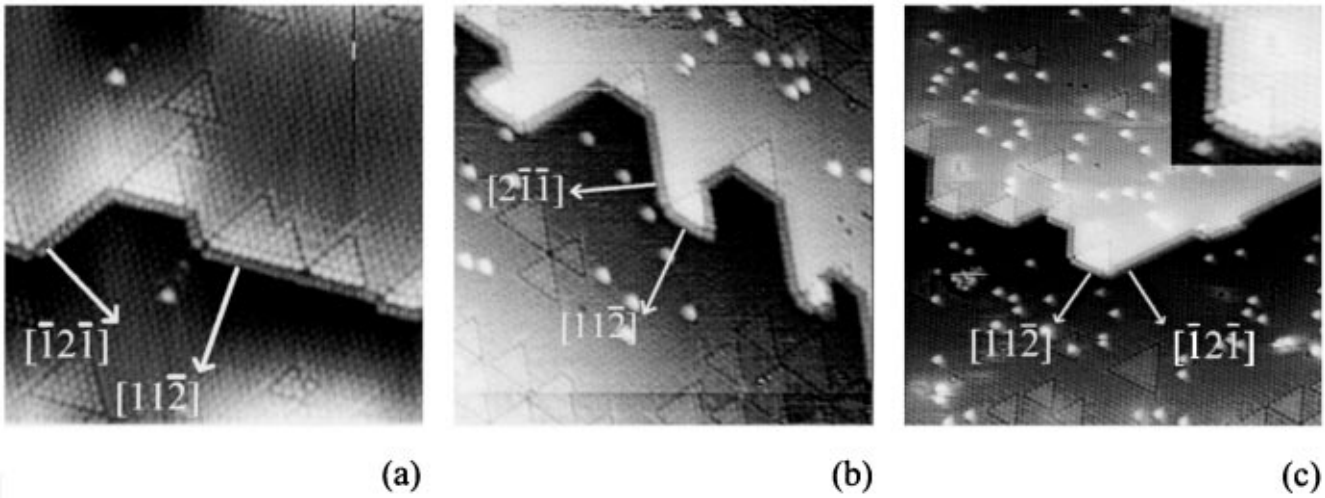

FIG. 2. Series of STM images of single bilayer steps of the Br-terminated Si(111)-(1 × 1) surface prepared by Br_2 exposure at ~400 °C (uncorrected for thermal drift). $\langle \bar{1}\,\bar{1}2\rangle$ steps have a bulk termination structure along their top terrace edges while $\langle 11\bar{2}\rangle$ steps are dressed by faulted triangular structures along the top terrace edge. (a) Area ~ (165 Å)^2, $V_{\text{sample}} = +2$ V, $I_{\text{tunnel}} = 0.48$ nA; (b) area ~ (230 Å)^2, $V_{\text{sample}} = +1.74$ V, $I_{\text{tunnel}} = 0.14$ nA; (c) area ~ (306 Å)^2, $V_{\text{sample}} = +2$ V, $I_{\text{tunnel}} = 0.10$ nA, inset: zoomed-in view to illustrate the same atomic structure for both sides of a 60° kink.

energy cost of the required stacking faults. Additionally, more recent results demonstrate that the *B*-type step edge structure is energetically unfavorable on Br-terminated Ge(111) substrates [10], indicating that this behavior is a general property of diamond lattices.

Despite the dramatic preference for *A*-type step edges, it is unclear why the *B*-type termination is precluded. We note, however, the electrostatic repulsion between negatively charged, monovalent Br atoms along the upper and lower terraces is more significant for the *B*-type step termination, compared to a rebonded *A*-type step structure. Moreover, the *B*-type step termination requires that each edge silicon atom of the upper terrace is bonded to a halogen atom, whereas every second silicon atom is bonded to a halogen for a rebonded *A*-type step. We speculate that either of these mechanisms might destabilize *B*-type steps, leading to their preferential loss under etching conditions and their inability to form under growth conditions. We anticipate that electronic structure calculations will provide insight into the relative stability of *A*- and *B*-type steps.

It is important to emphasize that the energy required to maintain stacking faults along $\langle 11\bar{2} \rangle$ steps is not insignificant. The energy difference between having faulted or unfaulted structures along the top step edges determined the overall shapes of $\langle \bar{1}\,\bar{1}2 \rangle$ and $\langle 11\bar{2} \rangle$ steps, shown in Fig. 2. In analogy with the interrelation between kinks and step structures on the Si(001)-(2 × 1) surface [11], removal of Si atoms from an *A*-type step edge results in some length of the *B*-type structure, and *vice versa*. For $\langle \bar{1}\,\bar{1}2 \rangle$ steps, such a kink would then require the formation of a stacking fault to convert back to an *A*-type structure and avoid formation of the unfavorable *B*-type edge structure. Since the energy of a faulted structure is larger than an unfaulted structure, kinks along $\langle \bar{1}\,\bar{1}2 \rangle$ steps are therefore unfavorable, yielding $\langle \bar{1}\,\bar{1}2 \rangle$ steps which are long and straight. Conversely, since kinks along $\langle 11\bar{2} \rangle$ steps reduce the stacking fault area, they are energetically favorable. Hence, $\langle 11\bar{2} \rangle$ steps have a jagged appearance, with many segments of $\langle \bar{1}\,\bar{1}2 \rangle$ steps incorporated, as shown in Fig. 2(c).

Faulted structures are not only seen at step edges, but also at the edges of islands. Figure 3 shows a large, triangular island formed from halogenated Si adatoms coalescing together on (1 × 1) regions of the surface [4]. These islands are analogous to CVD-grown structures. In instances where the island shape diverges from triangular, such as the truncated apex of the island in Fig. 3, faulted structures are incorporated that follow the same rules observed for the kinks and corners of step edges. Just as for step edges, stacking faults and dimer rows are created in the island to preserve the *A*-type atomic edge structure. Again, these faulted triangles cannot be remnants of the original surface's (7 × 7) domain, since these islands did not exist before the Br_2 exposure.

As further evidence of the strong preference of *A*-type edge structures, bilayer islands have a strong preference

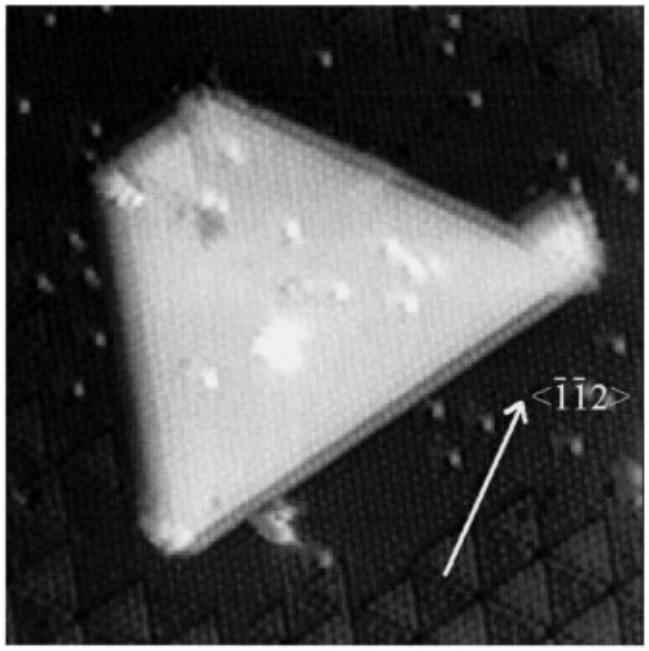

FIG. 3. STM image of an unfaulted triangular bilayer island on the Br-terminated Si(111) − (1 × 1) surface prepared by Br_2 exposure at ~400 °C (uncorrected for thermal drift). $\langle 11\bar{2} \rangle$ edges are dressed by faulted triangular structures, thereby maintaining the *A*-type step edge structure over the whole island perimeter. Area ~ (233 Å)^2, $V_{\text{sample}} = +1.92$ V, $I_{\text{tunnel}} = 1.0$ nA.

for being triangular, pointing in the $\langle 11\bar{2} \rangle$ directions, and having an unfaulted registry with respect to the underlying atomic layer. While triangular islands may be expected by considering the symmetry of the (1 × 1) structure, such considerations would allow for unfaulted islands pointing in both sets of directions. However, unfaulted islands pointing in the $\langle \bar{1}\,\bar{1}2 \rangle$ directions, which would necessarily have the *B*-type step structure, are never observed. Occasionally, small triangular islands are observed to be pointing in the $\langle \bar{1}\,\bar{1}2 \rangle$ direction, but, upon closer inspection, these islands are found to have the *A*-type step structure and a faulted registry with respect to the underlying layer. The small size and number of these faulted triangular islands is due to their higher energy relative to unfaulted islands. This faulted/unfaulted energy difference is also illustrated by the observation that, along $\langle 11\bar{2} \rangle$ step edges, typically there are many smaller faulted triangular structures rather than a single large triangle spanning the complete length of the step [Fig. 2(a)]. This reduces the total faulted area and hence the energy of the structure. Evidently, although the incorporation of the required stacking fault costs energy, more energy is gained by forming an *A*-type step edge.

The preference for the *A*-type step edge structure also is seen in the etching regime of the silicon-halogen system. Figure 4 is a STM image obtained after Br_2 exposure of the Si(111) surface while at 530 °C. The resulting etch

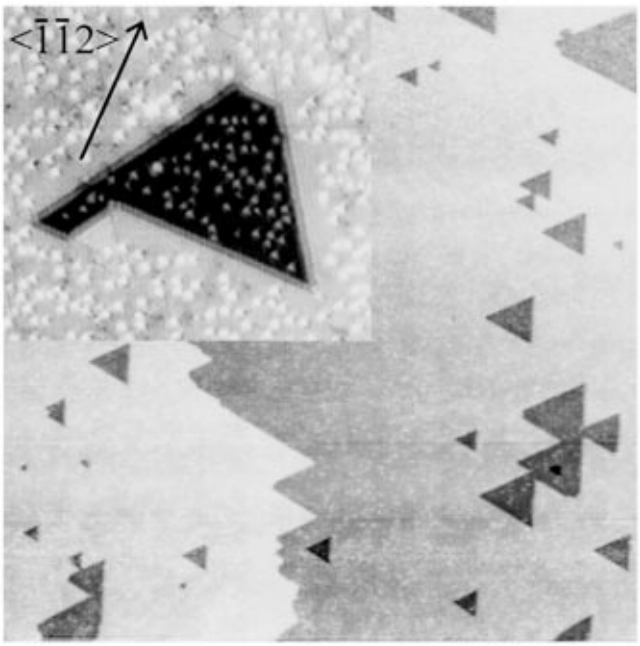

FIG. 4. STM image [area $\sim$ (5000 Å)^2, $V_{\text{sample}} = +1.96$ V, $I_{\text{tunnel}} = 1.0$ nA] of the Br terminated Si(111)-(1 $\times$ 1) surface after Br_2 exposure at $\sim$530 °C (uncorrected for thermal drift). The etch pits produced are triangular, and point in the $\langle \bar{1}\,\bar{1}2\rangle$ directions. Inset: Close-up view of one etch pit [area $\sim$ (263 $\times$ 238 Å), $V_{\text{sample}} = +1.88$ V, $I_{\text{tunnel}} = 1.0$ nA]. $\langle 11\bar{2}\rangle$ edges are dressed by faulted triangular structures, thereby maintaining the *A*-type step edge structure over the whole etch pit perimeter.

pits are clearly triangular with one dominant orientation, i.e., pointing in the $\langle \bar{1}\,\bar{1}2\rangle$ directions. Atomically resolved STM images (inset of Fig. 4) clearly show that, for the occasional $\langle 11\bar{2}\rangle$ etch pit edge, faulted structure are formed which allow the *A*-type step edge structure to be maintained along the entire perimeter of the etch pit.

In conclusion, steps in inequivalent crystallographic directions are usually assumed to have different atomic structures. However, this Letter has clearly shown that the bilayer steps of the Br-terminated Si(111)-(1 $\times$ 1) surface in the two principal crystallographic directions ($\langle \bar{1}\,\bar{1}2\rangle$ and $\langle 11\bar{2}\rangle$) have the same atomic *A*-type edge structure, due to the introduction of stacking faults along $\langle 11\bar{2}\rangle$ step edges. Similar results observed on Cl- and I-terminated Si surfaces, as well as for Br-terminated Ge substrates, indicate that this is a general property of halogen-passivated diamond lattices. This strong preference for the rebonded *A*-type step edge structure along both $\langle \bar{1}\,\bar{1}2\rangle$ and $\langle 11\bar{2}\rangle$ crystallographic directions determines the surface morphology of steps, islands, and etch pits for this system.

Financial support for this work has been provided by the National Science Foundation under Contracts No. DMR 9509790 and No. DMR 9413999, and is gratefully acknowledged.

*Present address: University of Virginia School of Law, 580 Massie Road, Charlottesville, Virginia 22903-1789
†Corresponding author

[1] R. J. Pechman, T. Moriwaki, J. H. Weaver, and G. S. Khoo, Surf. Sci. **341**, L1085 (1995).
[2] L. Andersohn, Th. Berke, U. Köhler, and B. Voightländer, J. Vac. Sci. Technol. **A14**, 312 (1996).
[3] U. Köhler, L. Andersohn, and B. Dahlheimer, Appl. Phys. A **57**, 491 (1993).
[4] B. S. Itchkawitz and J. J. Boland (to be published).
[5] J. J. Boland and J. S. Villarubia, Phys. Rev. B **41**, 9865 (1990).
[6] J. S. Villarubia and J. J. Boland, Phys. Rev. Lett. **63**, 306 (1989).
[7] F. Owman and P. Mårtensson, Surf. Sci. **324**, 211 (1995).
[8] While the local bonding is identical, the third nearest neighbor interactions of these two step orientations are different, as is expected for faulted structures.
[9] Since STM images cannot make a unique identification of step edge structures, the possibility of a doubly coordinated Br atom in the bridging bond site cannot be excluded. However, the STM images are clearly inconsistent with a dimerized structure for the $\langle \bar{1}\,\bar{1}2\rangle$ steps as described by Ref. [1].
[10] M. Fouchier, M. McEllistrem, and J. J. Boland, (to be published).
[11] B. S. Swartzentruber, Y.-W. Mo, R. Kariotis, M. G. Lagally, and M. B. Webb, Phys. Rev. Lett. **65**, 1913 (1990).